University of Massachusetts Amherst

ScholarWorks@UMass Amherst

Biology Department Faculty Publication Series

Biology

2007

A conserved role for kinesin-5 in plant mitosis

A Bannigan

WR Scheible

W Lukowitz

C Fagerstrom

P Wadsworth

See next page for additional authors

Follow this and additional works at: https://scholarworks.umass.edu/biology_faculty_pubs

Part of the Biology Commons

Recommended Citation

Bannigan, A; Scheible, WR; Lukowitz, W; Fagerstrom, C; Wadsworth, P; Somerville, C; and Baskin, TI, "A conserved role for kinesin-5 in plant mitosis" (2007). *Journal of Cell Science*. 14.
https://10.1242/jcs.009506

Authors

A Bannigan, WR Scheible, W Lukowitz, C Fagerstrom, P Wadsworth, C Somerville, and TI Baskin

A conserved role for kinesin-5 in plant mitosis

Alex Bannigan[1], Wolf-Rüdiger Scheible[2], Wolfgang Lukowitz[3], Carey Fagerstrom[1], Patricia Wadsworth[1], Chris Somerville[4] and Tobias I. Baskin[1],*

[1]Biology Department, University of Massachusetts, Amherst, MA 01003 USA
[2]Max Planck Institute for Molecular Plant Physiology, Science Park Golm, 14476 Potsdam, Germany
[3]Cold Spring Harbor Laboratory, 1 Bungtown Rd, Cold Spring Harbor, NY 11724, USA
[4]Carnegie Institution, Department of Plant Biology, Stanford, CA 94305, USA
*Author for correspondence (e-mail: baskin@bio.umass.edu)

Journal of Cell Science

Summary

The mitotic spindle of vascular plants is assembled and maintained by processes that remain poorly explored at a molecular level. Here, we report that AtKRP125c, one of four kinesin-5 motor proteins in arabidopsis, decorates microtubules throughout the cell cycle and appears to function in both interphase and mitosis. In a temperature-sensitive mutant, interphase cortical microtubules are disorganized at the restrictive temperature and mitotic spindles are massively disrupted, consistent with a defect in the stabilization of anti-parallel microtubules in the spindle midzone, as previously described in kinesin-5 mutants from animals and yeast. AtKRP125c introduced into mammalian epithelial cells by transfection decorates microtubules throughout the cell cycle but is unable to complement the loss of the endogenous kinesin-5 motor (Eg5). These results are among the first reports of any motor with a major role in anastral spindle structure in plants and demonstrate that the conservation of kinesin-5 motor function throughout eukaryotes extends to vascular plants.

Supplementary material available online at
http://jcs.biologists.org/cgi/content/full/120/16/2819/DC1

Introduction

The mitotic spindle separates replicated chromosomes, a hallmark process for the eukaryotic cell. Early observations on the mitotic spindle revealed that the spindle is reliably a bipolar structure in all eukaryotes and differs among taxa primarily in the nature of the poles. In particular, most animal spindles have focused poles that contain centrosomes, whereas most vascular plant spindles have broad, acentrosomal, poles (Baskin and Cande, 1990; Mineyuki, 2007). According to the 'diffuse centrosome' model (Mazia, 1984), the function of the spindle pole is spread across a broad region at each end of the plant spindle, a concept that has reconciled the spindles of plant and animal cells, despite their different polar morphology.

Morphological studies of the spindle have been succeeded by molecular studies (Sharp et al., 2000b; Gadde and Heald, 2004). These have revealed that the bipolar symmetry of the spindle requires opposing forces, generated by motor proteins pushing in opposite directions on spindle microtubules. At the mid-zone, plus-end-directed motors push the poles apart by cross-linking anti-parallel microtubules and walking to their plus ends; while at the pole, minus-end-directed motors draw the spindle halves together and focus the poles. In addition to revealing the force balance, molecular studies have identified many of the responsible proteins. The animal spindle pole is focused by cytoplasmic dynein and minus-end-directed kinesins, whereas the plus-end-directed activity in the midzone of animal and yeast spindles is exerted predominantly by members of the kinesin-5 family (e.g. Eg5, BIMC).

Molecular studies on the mitotic spindle are relatively advanced for animals and fungi but they are just beginning for plants. Genomic studies have revealed that vascular plants, with the loss of ciliated sperm, also lost cytoplasmic dynein, and families of minus-end-directed kinesins have undergone extensive radiation (Reddy and Day, 2001). Mutation in either of two minus-end-directed kinesins in arabidopsis gives rise to spindles with slightly broader poles, indicating a supporting role for these motors in polar function (Marcus et al., 2003; Ambrose et al., 2005). In fact, all types of kinesin motors have proliferated in plants: there are 61 annotated kinesins in the arabidopsis genome (Lee and Liu, 2004). The specific motors playing major roles in the structure and function of the plant mitotic spindle remain to be elucidated.

Of particular interest, because of their conserved and pre-eminent role in the animal and yeast spindle, are kinesin-5 motors. These kinesins are N-terminal, plus-end-directed motors, implicated in crosslinking anti-parallel microtubules and sliding them apart. They are thought to assemble into homotetramers (Goldstein and Philp, 1999) and walk simultaneously towards the plus ends of both microtubules that they crosslink (Kapitein et al., 2005). Perturbation of kinesin-5 motors in animals or yeast has catastrophic consequences for spindle structure, typically more so than the loss of other mitotic motors (Sharp et al., 2000b; Goldstein and Philp, 1999; Sawin et al., 1992; Sawin and Mitchison, 1995; Heck et al., 1993; Endow, 1999; Sharp et al., 1999; Kapoor et al., 2000). Loss or reduction of kinesin-5 function is characterized by the formation of mono-polar spindles and cell cycle arrest (Sawin et al., 1992; Heck et al., 1993; Endow, 1999; Sharp et al., 1999; Kapoor et al., 2000; O'Connell et al., 1993; Sawin and Mitchison, 1995).

Kinesin-5 motors are present in plants (Reddy and Day, 2001). In tobacco, the kinesin-5, TKRP125, was inferred to be involved in separating anti-parallel microtubules in the cytokinetic organelle, the phragmoplast (Asada et al., 1997). In the arabidopsis genome, four sequences have been annotated as kinesin-5 members, whereas in animal genomes kinesin-5 is present usually as a single-copy gene. These plant proteins have similarity to mammalian Eg5, particularly in the motor domain, but also throughout the rest of the sequence. It is unknown whether any or all of these motors function in the plant mitotic spindle or whether, with their duplication, they have acquired new functions.

The temperature-sensitive arabidopsis mutant, *radially swollen7* (*rsw7*), was originally described as having reduced growth anisotropy (i.e. root swelling) despite normal microtubule and cellulose microfibril organization (Wiedemeier et al., 2002). It was hypothesized that root swelling in *rsw7* was caused by a defect in cell wall composition. However, we report here that *RSW7* encodes one of the four arabidopsis kinesin-5 class kinesins, AtKRP125c, and that this protein plays an essential role at mitosis. We show that the mutation causes mitotic spindle collapse similar to that described in animal and fungal cells with compromised kinesin-5 function. Unlike other kinesin-5 motors, AtKRP125c appears also to function at interphase. Characterization of AtKRP125c demonstrates the central role of kinesin-5 proteins in mitosis throughout eukaryotes.

Results

RSW7 encodes a kinesin-5, AtKRP125c

The *RSW7* gene was identified by recombinational mapping based on the conditional root-swelling phenotype of *rsw7* (Fig. 1). The candidate gene, *At2g28620*, belongs to the kinesin-5 family, and is known as AtKRP125c (Reddy and Day, 2001). A single nucleotide polymorphism (G to A, at position 50835 on AGI BAC T8O18; GenBank accession AC007171) was found in the *rsw7* mutant in the fourth exon. The mutation replaces glutamate with lysine at position E280, predicted to be in β-six, near the tip of the so-called arrowhead of the kinesin motor domain (Turner et al., 2001). Complementation of the *rsw7* root phenotype was achieved by transforming *rsw7* with an 11.8 kb genomic *Apa*I fragment containing the kinesin-5 gene, ~5 kb of 5′ and ~2 kb of 3′ untranslated regions. The T2 progeny segregated *rsw7* and wild-type phenotypes in a ratio indistinguishable from 1:3 (Fig. 1E). Recent re-annotation revealed that the 5′ sequence also contains a small expressed gene of unknown function, *At2g28625*; however, sequencing the entire predicted coding sequence of this gene from *rsw7* showed no mutations. Furthermore, a strong mutation in AtKRP125c, termed *loophole* (*lph*), was independently recovered from a visual screen for mutations disrupting division in the embryo. This allele harbors a substitution in a highly conserved residue of the kinesin catalytic core domain (glycine at position 357 to arginine) and fails to complement the *rsw7* phenotype (W.L. and C.S., unpublished).

AtKRP125c localizes to all microtubule arrays throughout the cell cycle

To examine localization of the protein, we transformed *rsw7* plants with a genomic AtKRP125c-GFP (C-terminal) construct, which complemented the mutant phenotype, and we
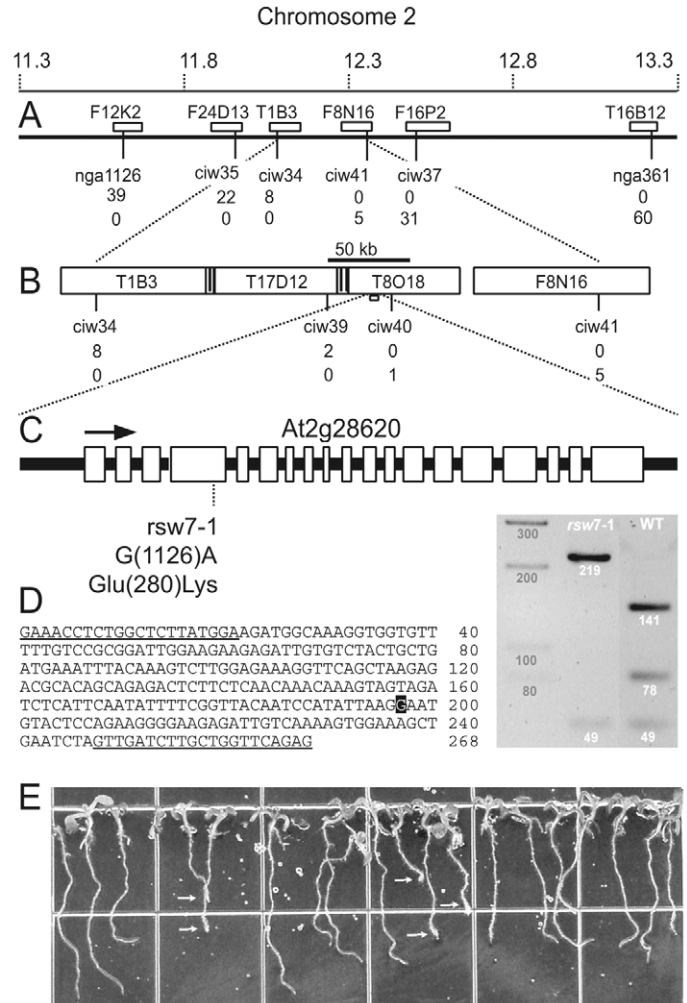

Fig. 1. Identification of RSW7 by recombinational mapping, candidate gene sequencing and complementation. (A) Representation of a part of arabidopsis chromosome 2 showing the positions of SSLP markers used in mapping. White boxes represent AGI-BAC clones. Numbers are recombination events for each marker in a total of 1920 examined chromosomes. (B) Enlargement of the region between SSLP-markers ciw34 and ciw41, showing the names of BAC clones, as well as the position and the number of recombinants. The candidate gene, *At2g28620*, is depicted as a white box. (C) Exon-intron structure of the kinesin-like gene *At2g28620* and the single nucleotide polymorphism in *rsw7* (G in wild-type to A in *rsw7*) found in the fourth exon. Base and amino acid numbers indicate position in the gene. (D) Identification of *rsw7* plants by PCR. The polymorphism destroys a *Bsl*I restriction site (CCN7GG) in *rsw7*, therefore representing a CAPS marker (primers shown as underlined sequences). Base numbers on right indicate position in amplified sequence. The gel shows a DNA standard (left), *Bsl*I digests of *rsw7* (middle) and wild-type (right) PCR products. The predicted sizes of the digested fragments are shown. (E) Complementation of the *rsw7* root phenotype with the wild-type *At2g28620* gene. Shown is the segregation in the T2 progeny of an *rsw7* mutant transformed with an 11.8 kb genomic fragment containing the *AtKRP125c* gene. Arrows indicate T2 plants with *rsw7* phenotype.

bred a pure line from phenotypically wild-type plants (Fig. 2A). Confocal microscopy revealed that AtKRP125c-GFP
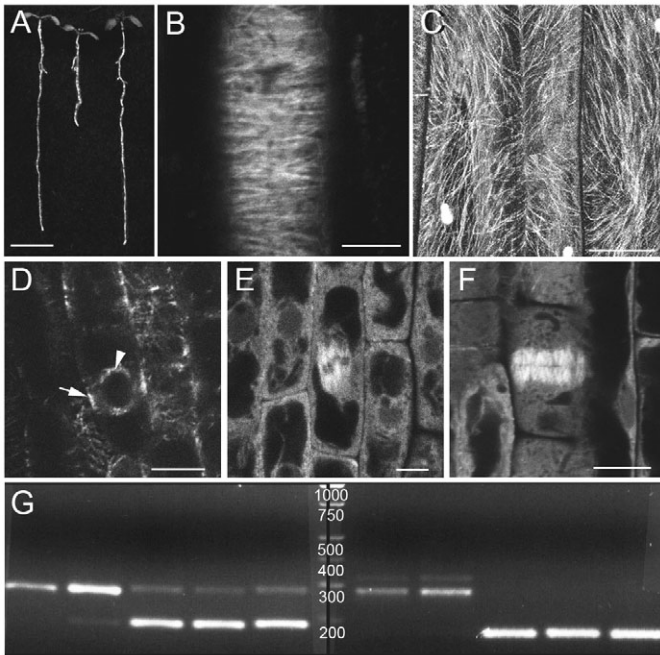
Fig. 2. AtKRP125c localization and expression.
(A) Complementation of the *rsw7* phenotype by transformation with AtKRP125c-GFP: 1-week-old wild-type (left), *rsw7* (middle) and complemented *rsw7* (right) seedlings grown at 19°C. Bar, 5 mm. (B-F) Confocal micrographs showing AtKRP125c-GFP in living cells of complemented *rsw7* plants. AtKRP125c-GFP decorates cortical microtubules in the root (B) and hypocotyl (C), and division figures in the root, including preprophase band (D, arrow) and prophase spindle (D, arrowhead), mitotic spindle (E), and phragmoplast (F). Bars, 5 μm. (G) RT-PCR on RNA from whole 2-week-old seedlings (35 cycles). Left-hand gel: EF1-α (loading control); right-hand gel: AtKRP125c. The lane order is the same in both. Lane 1: Col genomic DNA. Lane 2: AtKRP125c-GFP genomic DNA. Lane 3: Col cDNA. Lane 4: *rsw7* cDNA. Lane 5: AtKRP125c-GFP cDNA. Size standards shown in the middle.

localized abundantly to all microtubule arrays in the root tip and to cortical microtubules in the hypocotyl (Fig. 2B-F). Microtubules appeared to function normally when decorated with the construct. Preferential plus-end localization was not seen; instead, fluorescence was uniform along the length of microtubules in all of the arrays. The construct was expressed under the native AtKRP125c promoter, and no evidence of overexpression was found in an RT-PCR-based comparison of mRNA levels between wild-type and transgenic lines (Fig. 2G). The abundant localization of AtKRP125c-GFP to all microtubule arrays throughout the cell cycle therefore appears to reflect the distribution of the native protein.

AtKRP125c is necessary for cortical microtubule organization

In light of the localization results, we looked at interphase microtubule orientation and the mutant's growth response to microtubule inhibitors. Close inspection of the cortical microtubule array in *rsw7* showed disorganization at the restrictive temperature (Fig. 3A-D). In cells of the elongation zone in fixed and immunolabeled roots, the interphase array was characteristically parallel, and transverse to the long axis
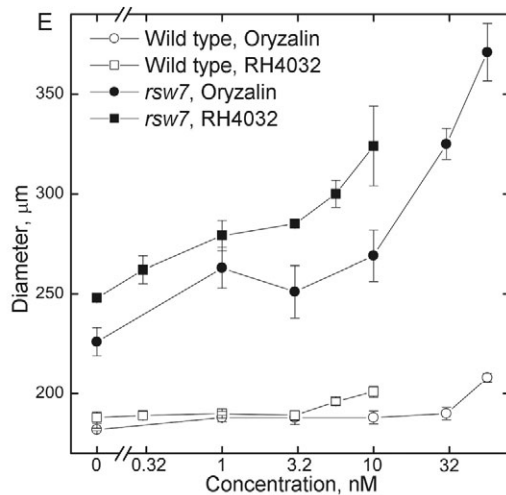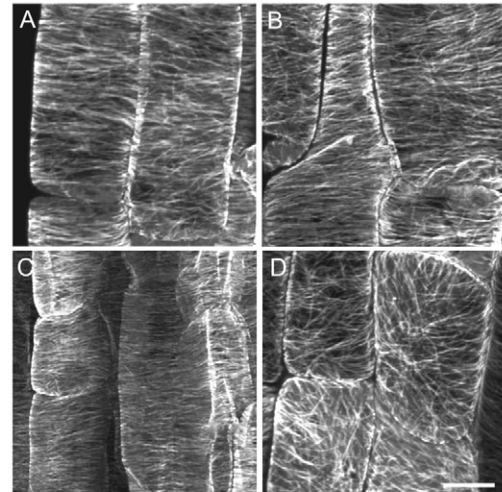

Fig. 3. Interphase microtubules in *rsw7* root tip cells. (A-D) Confocal immunofluorescence micrographs of microtubules in fixed and immunolabeled 7-day-old root epidermal cells. (A,C) Wild type, (B,D) *rsw7*; top panels (A,B) grown at the permissive temperature (19°C); lower panels (C,D) grown at 19°C for 6 days and then exposed to the restrictive temperature (30°C) for 12 hours. Images representative of 6-10 roots, per treatment, examined in four different experiments. Bar, 5 μm. (E) Dose-response curve for root diameter as a function of concentration of two different microtubule inhibitors, oryzalin (circles) and RH-4032 (squares). Data presented as mean ± s.e.m. of three replicate plates. The *x* axis (concentration) is logarithmic. In the absence of inhibitor, the root diameter of *rsw7* plants is significantly greater than that of the wild type because the *rsw7* phenotype is partially expressed at 19°C (Wiedemeier et al., 2002).

of the root in *rsw7* plants grown at 19°C as well as in wild-type plants grown at both 19°C and 30°C; however, in *rsw7* plants after 12-24 hours at 30°C, the microtubules in many epidermal cells became noticeably disorganized and this corresponded with the swelling of the root tip. This was confirmed with GFP-tubulin-expressing *rsw7* lines (data not shown).

To explore the interphase phenotype further, we assayed the sensitivity of *rsw7* to microtubule inhibitors. Two microtubule depolymerizing drugs from distinct chemical classes were chosen (oryzalin and RH4032) and the concentrations used

were at and below the threshold for causing root swelling in the wild type (Baskin et al., 2004). For both compounds, the threshold for swelling was decreased in *rsw7* plants compared with that of the wild type by approximately an order of magnitude (Fig. 3E). Taken together, our data suggest that AtKRP125c is involved with microtubule function at interphase.

Loss of AtKRP125c severely compromises spindle structure and cytokinesis

Because kinesin-5 motors are known to participate in mitosis in other organisms, we examined mitotic and cytokinetic arrays in *rsw7* cells, both in fixed and immunolabeled roots and using
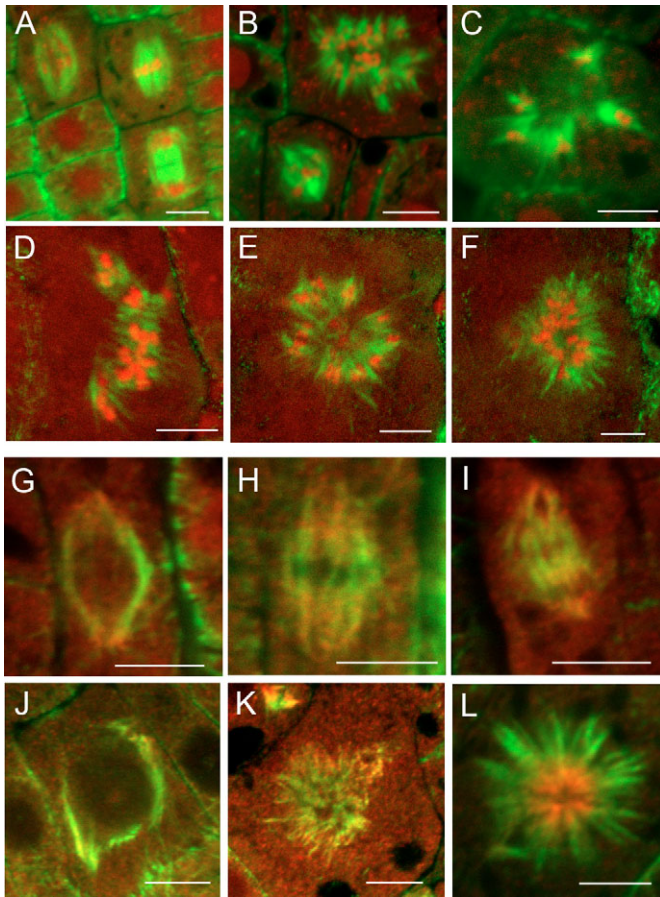
a GFP-tubulin reporter line. In *rsw7* plants fixed at 19°C, the majority of spindles were similar to wild-type spindles (Fig. 4A), although abnormalities similar to those described below for plants at 30°C were seen occasionally (Fig. 4B). After 12-24 hours at 30°C, most spindles were deformed, unfocussed, mono-polar or fragmented, with chromosomes failing to align at the metaphase plate (Fig. 4C-F). In mono-polar spindles, chromosomes could be seen in a central mass or spread around the periphery (Fig. 4E,F).

Spindle stages and the polarity of spindle microtubules in *rsw7* were assessed by double labeling for α- and γ-tubulin. In the wild type, γ-tubulin localized strongly to the poles at prophase and anaphase, but was dispersed throughout the spindle at prometaphase and metaphase (Fig. 4G-I). This is similar to γ-tubulin distributions reported previously for other plants (Liu et al., 1993; Dibbayawan et al., 2001; Brown et al., 2004). In *rsw7*, γ-tubulin was seen at the poles in prophase, throughout the spindle in disorganized apolar spindles, and concentrated at the centre of mono-polar spindles (Fig. 4J-L). This implies that the diffuse, multi-polar spindles were in prometaphase or metaphase whereas mono-polar spindles were probably at anaphase, with a pole at the centre.

In fixed tissue, pre-prophase bands and phragmoplasts resembled those of the wild type (Fig. 5), at both the permissive and restrictive temperatures. Defects in cytokinesis were often seen, particularly after prolonged exposure to the restrictive temperature, including cell wall stubs, enlarged cells, multiple nuclei, and nuclei partially bisected by an incomplete cell wall. However, although phragmoplasts were often misplaced or wavy, microtubule organization within them appeared to be
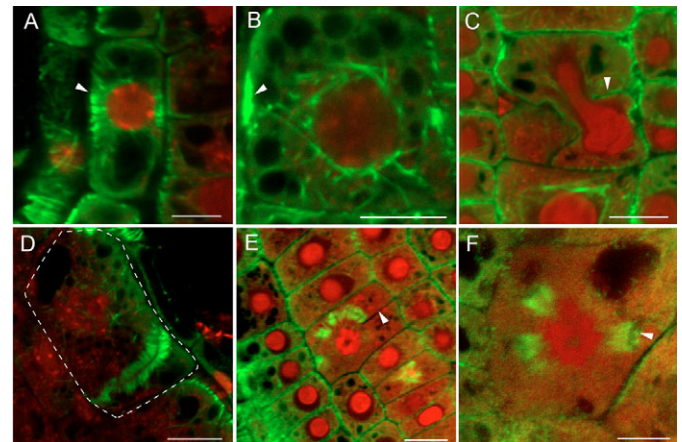

Fig. 4. Confocal micrographs of fixed cells with immunolabeled spindles. (A-F) Spindles double labeled for microtubules (green) and DNA (red). (A) Wild-type cells. Typical bipolar spindles in (clockwise from the upper left) anaphase, metaphase and telophase. (B) *rsw7* cells grown at 19°C. Most spindles resembled those of the wild type, but a few were aberrant, such as the multi-polar spindle at the top of the panel. (C-F) *rsw7* cells exposed to 30°C for 16-24 hours illustrating the range of morphologies, including radial (C,E,F) and linear (D). Radial spindles varied from compact (F) to diffuse (C) and chromosomes were seen either at the centre or periphery of the radial spindle. (G-L) Double labeling for α-tubulin (green) and γ-tubulin (red). In the wild type (G-I), γ-tubulin is concentrated at the poles at prophase (G) and anaphase (I), but dispersed though the spindle at metaphase (H). In *rsw7* (J-L), γ-tubulin is focused at the poles at prophase (J), spread throughout the diffuse spindles (K), and at the centre of compact, radial spindles (L). Bars, 5 μm.

Fig. 5. Pre-prophase bands and phragmoplasts in *rsw7* cells. Confocal micrographs of preprophase bands and phragmoplasts in cells of *rsw7* plants exposed to the restrictive temperature for 24 hours (A-D) and 6 hours (E,F) prior to fixation. (A,B) Preprophase bands. (C) Cell with an enlarged nucleus and incomplete cross wall. (D) Cell with curved and asymmetrically placed, but structurally normal, phragmoplast. The cell margin is marked with a dashed line. (E) Cell with an aborted cell wall (arrowhead) and unusually deployed phragmoplast fragments. (F) Cell with central DNA mass and radially deployed phragmoplast fragments, possibly reflecting a stage following a spindle as shown in Fig. 4L. Such residual microtubule structures sometimes appeared to be associated with fragments of cell plate (arrowhead). Bars, A,B 5 μm; C-F 10 μm.

relatively unaffected (Fig. 5D,E). Instances of failed cytokinesis probably followed from failed disjunction. During live imaging of GFP-tubulin, in cells with mildly abnormal spindles, phragmoplasts were able to form successfully, but the formation of a normal phragmoplast was never seen following complete spindle collapse. Occasionally in fixed cells, one-sided phragmoplasts were seen, which appeared to form small sections of cell plate (Fig. 5F).

Time-lapse imaging of spindles in *rsw7* plants expressing GFP-tubulin revealed that, whereas some spindles were able to go through mitosis fairly normally after 6-7 hours at 30°C (supplementary material Movie 1), many failed to complete anaphase. Typically, after a prolonged prometaphase, the spindle poles collapsed towards each other, leaving the plus ends of the spindle microtubules pointing outwards (Fig. 6 and supplementary material Movie 2). The cell cycle appeared to continue after spindle collapse. In many cases, the spindle microtubules were observed moving away from a central DNA mass, towards the edges of the cell in an apparent attempt to construct a phragmoplast (Fig. 6, 12:00). When these microtubules reached the parent wall, rather than reaching another half-phragmoplast, they disappeared. In plants exposed to 30°C for 24 hours or more, spindles rarely had a normal structure. Usually, they were diffuse, churning arrays, unable to focus at the poles, align chromosomes at the metaphase plate or separate the chromosomes (supplementary material Movie 3). Some spindles such as these were observed for up to 20 minutes without a recognizable transition to anaphase.

AtKRP125c fails to rescue spindles in animal cells with inhibited Eg5 function

To assess the degree of conservation of kinesin-5 function between plants and animals, we first used monastrol, a small, organic molecule known to inhibit mammalian Eg5 (Kapoor et al., 2000). Application of up to 200 μM monastrol to wild-type arabidopsis roots for 1-24 hours failed to induce formation of mono-polar spindles, although root elongation was mildly inhibited and the frequency of dividing cells was lowered.

As a more stringent test, we transfected porcine kidney epithelial (LLC-Pk1) cells with an AtKRP125c-myc construct and used immunocytochemistry to observe the results in fixed cells. AtKRP125c localized to microtubules in animal cells (Fig. 7A,C) and transfected cells were not detectably impaired in their progress through mitosis. As in plants, AtKRP125c decorated microtubules abundantly in both interphase and mitotic cells, without preferential plus-end accumulation. By contrast, antibodies to Eg5 only labeled microtubules in mitotic cells, particularly at the spindle poles (Fig. 7B,D).

To reduce Eg5 function, we either treated LLC-Pk1 cells with monastrol (given the apparent insensitivity of AtKRP125c) or co-transfected cells with a hairpin RNAi construct against Eg5 (Weil et al., 2002). In both cases, prominent monopolar spindles formed, which led to cell cycle arrest (Fig. 7E,F). In cells transfected with the AtKRP125c-
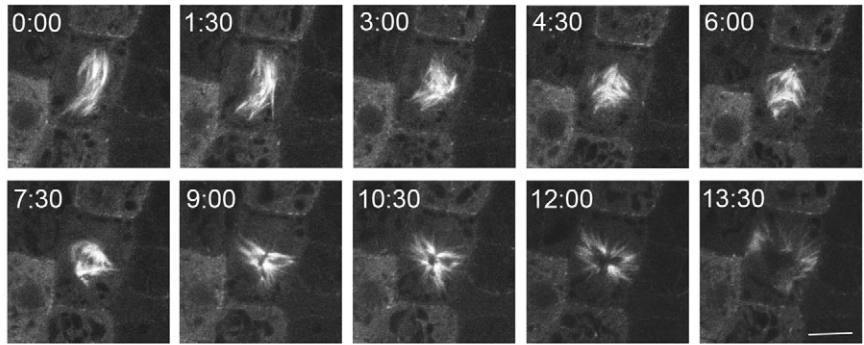

Fig. 6. Mitosis in live *rsw7* cells. Single frames from an image sequence of GFP-tubulin in the *rsw7* background. For the complete sequence see Movie 2 in supplementary material. The seedling had been exposed to 30°C for approximately 7 hours by time zero (min:sec, in upper left). This spindle was more or less bipolar to start with, although the poles were less focused than normal. The spindle appeared to be in a prometaphase-like state (0 to 3:00) before the poles rapidly collapsed towards each other (6:00 to 10:30). After a pause in the monopolar configuration, the microtubules migrated away from the poles towards the edges of the cell (12:00 to 13:30), leaving the chromosomes at the centre (visible as a dark mass). Bar, 5 μm.

myc construct, there was no significant increase in the number of cells with bipolar spindles (Table 1, Fig. 7G,H), indicating that, despite binding to microtubules, AtKRP125c did not rescue Eg5 loss of function in animal cells.

Discussion
The family of kinesin-5 motors in plants
We show here that the kinesin-5 motor, AtKRP125c, is crucial for mitosis in arabidopsis roots. The pioneer kinesin-5 in plants was purified from tobacco suspension-cultured cells and named tobacco kinesin-related peptide 125 (TKRP125) (Asada et al., 1997). TKRP125 was shown to have plus-end-directed motility in vitro, to be present in the spindle and phragmoplast and was hypothesized to function at their midzones. A related polypeptide (DcKRP120) has been isolated from the cold-resistant cytoskeleton of carrot (*Daucus carota*) suspension culture cells, and also binds microtubules, especially during mitosis (Barroso et al., 2000). In arabidopsis, there are four

Table 1. Frequency of monopolar spindles in LLC-Pk1 cells

Treatment	Monopoles	*P* value (1 d.f.)*
Untreated	0/67 (0%)	
AtKRP125c construct	0/520 (0%)	
Monastrol	116/132 (86.2%)	4.08
Monastrol + AtKRP125c	479/514 (93.2%)	
Eg5 RNAi	1773/1837 (96.5%)	4.12
Eg5 RNAi + AtKRP125c	1638/1676 (97.7%)	

*Significance $P<0.01=6.63$.
Data show the number of monopolar spindles counted over the total number of spindles, with the percentages in parentheses. In cells transfected with AtKRP125c only, all mitotic cells were counted. In cells co-transfected with AtKRP125c-myc and the Eg5 hairpin constructs, only cells that were Eg5 knocked-down, as judged by immunolabeling, were counted. Chi-squared tests showed no significant increase in the proportion of bipolar spindles in cells transfected with the AtKRP125c-myc construct compared with the corresponding control.
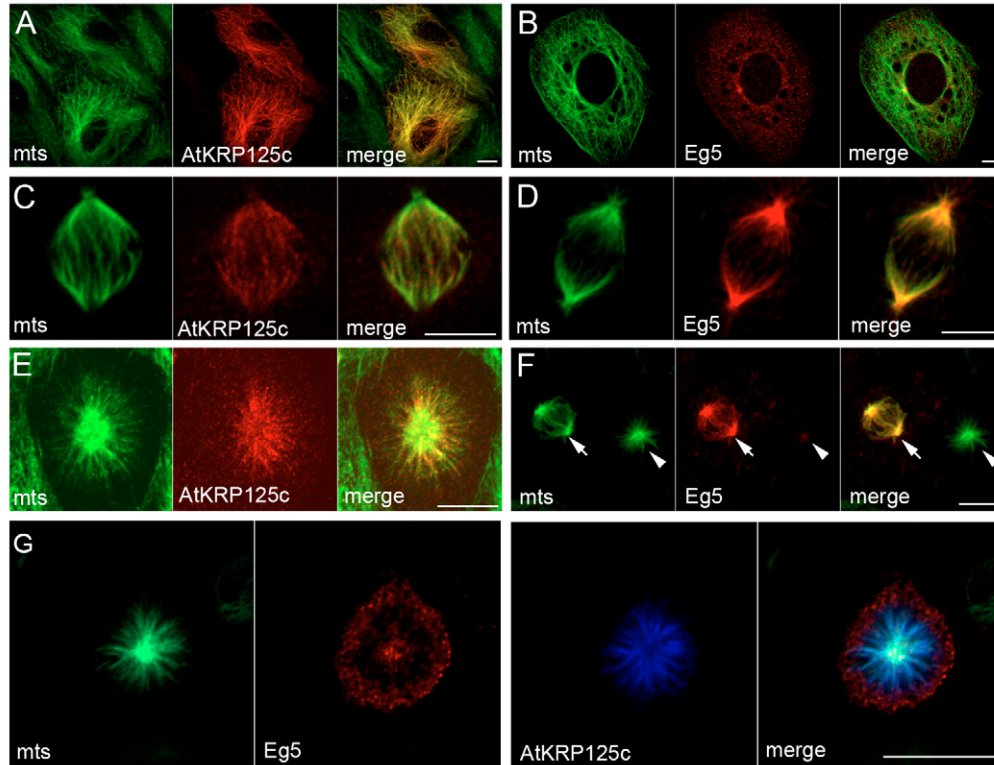
Fig. 7. Eg5 and AtKRP125c in fixed animal epithelial cells. (A,B) Interphase. AtKRP125c-myc localized to microtubules in LLC-Pk1 cells at interphase, whereas Eg5 did not. (C,D) Metaphase. Both AtKRP125c-myc and Eg5 were strongly localized to the spindle in mitotic cells. (E) Treatment of LLC-Pk1 cells with monastrol caused the formation of monopolar spindles and cell cycle arrest, which was not affected by the presence of AtKRP125c-myc. (F,G) Mitotic LLC-Pk1 cells transfected with a hairpin construct against Eg5 were clearly visible by the presence of monopolar spindles and diminished Eg5 labeling (F, arrowheads), whereas cells that were not knocked down had bipolar spindles that labeled strongly for Eg5 (F, arrows). In cells co-transfected with the Eg5 hairpin construct and the AtKRP125c-Myc construct (G), the great majority of spindles were monopolar, despite AtKRP125c binding to spindle microtubules. Bar, 10 μm.

kinesin-5 family motors (Reddy and Day, 2001), and because of the primacy of the tobacco work, three of the sequences were annotated as AtKRP125 a, b and c, and the fourth was named AtF16L2. The sequence with the greatest similarity to the tobacco protein is AtKRP125b (Reddy and Day, 2001).

Given these four kinesin-5 genes, it is reasonable to predict some functional redundancy, especially since *AtKRP125a, b* and *c* are all upregulated during mitosis (Vanstraelen et al., 2006). The persistence of some normal spindles in *rsw7* at the restrictive temperature might indicate partial redundancy between AtKRP125c and another kinesin-5 motor, or with structural spindle proteins, such as AtMAP65, which localizes to the spindle midline at anaphase (Mao et al., 2005). However, another mutant allele in *AtKRP125c*, *loophole*, causes severe cell division defects in pollen development and embryogenesis (W.L., unpublished data), which implies either a lack of redundancy, or dominance of AtKRP125c in early development. Because kinesin-5 motors in animals and yeast function as tetramers, the possibility exists that the native motor in arabidopsis comprises polypeptides from more than one gene. We have preliminary results showing that plants homozygous for T-DNA insertions in exons of two of the other kinesin-5 genes, *AtKRP125a* and *AtKRP125b*, have normal mitosis, suggesting that these motors function independently of AtKRP125c. However, we have so far failed to isolate any

plants homozygous for T-DNA insertions in the fourth kinesin-5 gene, *AtF16L2*, which hints that it has an essential function in arabidopsis. In the motor domain, AtKRP125c is 85.8% identical to AtF16L2 (compared with 69.3% and 78.6% identity to AtKRP125a and b, respectively), and therefore could plausibly function as a heterotetramer specifically with AtF16L2.

The four kinesin-5 motors might be explained partly by specialization between spindle and phragmoplast. It appears that problems with constructing phragmoplasts and cell plates seen in *rsw7* are the result of abnormal spindle formation, rather than cytokinesis defects per se. The correct formation of the phragmoplast is likely to depend on the placement of two reforming nuclei on either side of the division plane (Brown and Lemmon, 2001). Given that the phragmoplast requires a stable midzone through which microtubules move toward their minus ends (Asada et al., 1991), and that the phragmoplast evolved in the plant lineage, it is reasonable that some of the kinesin-5 duplication represents specialization for cytokinesis.

Function of AtKRP125c
We show here that, in arabidopsis, the kinesin-5 AtKRP125c plays a pivotal role in stabilizing the mitotic spindle. In time-lapse imaging of GFP-tubulin in *rsw7* at 30°C, spindle collapse was observed in the majority of spindles monitored, and even

in many spindles that started with relatively normal structure (Fig. 6), consistent with a weak midzone. The behaviour of spindles as seen in these movies was similar to descriptions of spindles in animal cells treated with an anti-BimC antibody (Sharp et al., 1999) or with monastrol (Kapoor et al., 2000).

In *rsw7* cells, microtubules often moved away from the centre of the collapsed spindle towards the edges of the cell, as though attempting to form a phragmoplast. Some of these microtubule clusters appeared to be associated with chromatin or cell plate fragments. This suggests that the disrupted spindles do not cause metaphase arrest, as they do in animal cells. A further indication that metaphase is not arrested in *rsw7* at 30°C is offered by the fact that the mitotic index did not increase over time and the occurrence of enlarged, sometimes multinucleate, cells in interphase.

Although kinesins that have major roles at cytokinesis have been identified in plants, to our knowledge, this is the first report of a kinesin mutant with a widespread alteration of mitotic spindle architecture. The kinesin mutants *atk1* (Marcus et al., 2003) and *atk5* (Ambrose et al., 2005) each lack a minus-end-directed kinesin and have mild phenotypes, characterized by slightly broadened spindles, although the defect in *atk1* is more severe at meiosis. Disrupted spindles, somewhat similar to those of *rsw7*, have been reported previously in broad bean (*Vicia faba*) roots treated to inhibit cyclin-dependent kinases (Binarová et al., 1998), consistent with AtKRP125c, like animal kinesin-5, requiring phosphorylation for activity (Blangy et al., 1995).

Along with its obvious role at mitosis, a role for AtKRP125c in organizing the cortical array during interphase is suggested by localization of AtKRP125c-GFP to cortical microtubules, the hypersensitivity of *rsw7* to anti-microtubule drugs, and the observation that interphase microtubules are disorganized in *rsw7* at the restrictive temperature. Although disorganization of cortical microtubules fits the root-swelling phenotype of *rsw7*, it was reported previously that cortical microtubules in *rsw7* and wild type were indistinguishable (Wiedemeier et al., 2002). The reason for the discrepancy is not clear. Wiedemeier et al. mainly examined microtubules in methacrylate sections, in which the cortical array is glimpsed in small patches because of the irregular cell shapes, hindering assessment of overall microtubule organization (Wiedemeier et al., 2002). Unlike other characterized kinesin-5 motors, AtKRP125c may play a direct role in microtubule organization at interphase; alternatively, disorganized microtubules and misshapen cells at interphase could be a secondary effect of an abnormal transition through M phase. The localization of AtKRP125c-GFP to interphase microtubules does not necessarily indicate its activity there, and further studies will be needed to identify the exact cause of the interphase phenotype in *rsw7*.

Comparison of kinesin-5 function in animals and plants

Overall, the defective spindle architecture seen here in *rsw7* is similar to that reported when kinesin-5 function is inhibited in animals and fungi (Endow, 1999; Sharp et al., 2000a) and suggests that the function of this motor has been conserved widely among eukaryotes (Lawrence et al., 2002). However, the kinesin-5 family members have diverged to some extent. The AtKRP125c protein was unable to rescue the loss of Eg5 activity in transfected mammalian epithelial cells (Fig. 7). The most likely explanation for this failure to complement loss of Eg5 is that AtKRP125c can effectively bind microtubules on its own but requires a plant-specific partner, whether a kinase or another member of the kinesin-5 family, to enable its motor activity.

In animal cells, the loss of kinesin-5 function is phenocopied by monastrol treatment (Kapoor et al., 2000), but this was not the case in arabidopsis. An alignment of the motor domains of Eg5 and AtKRP125c shows the latter has an elongated L5 loop, which would be expected to lower the affinity of monastrol binding (DeBonis et al., 2003; Maliga and Mitchison, 2006). Interestingly, in the brown alga, *Silvetia compresa,* monastrol causes formation of cytasters, multi-polar and mono-polar spindles, and leads to cell-cycle arrest (Peters and Kropf, 2006). Other cytological aspects of these algae are somewhat animal-like, suggesting an intermediate relationship to animals and higher plants (Katsaros et al., 2006).

AtKRP125c-GFP localized abundantly to the whole length of microtubules at all stages of the cell cycle in transformed plants: the cortical interphase array, pre-prophase band, spindle and phragmoplast. This was surprising in light of the restricted distribution pattern reported for other kinesin-5 motors. In plants, tobacco TKRP125 and carrot DcKRP120 localize predominantly to the spindle and phragmoplast, and preferentially to their equator, which is enriched for plus ends (Asada et al., 1997; Barroso et al., 2000). It is possible that in arabidopsis, AtKRP125c is present on all microtubules, but is specifically activated, perhaps by cell-cycle-regulated phosphorylation, in regions of microtubule overlap, such as the spindle midzone, at which point it gains motor activity and walks towards the microtubule plus ends.

In mammalian cells, antibodies to Eg5 strongly label the spindle, and paradoxically the signal is concentrated at the poles, but do not label interphase microtubules (Fig. 7) (Sawin et al., 1992; Sawin and Mitchison, 1995; Wadsworth et al., 2005). By contrast, the AtKRP125c-Myc construct labeled all arrays in transfected animal cells evenly. This could be the result of overexpression, but Eg5-Myc overexpressed in animal cells does not localize to interphase arrays (Sawin and Mitchison, 1995). In transformed arabidopsis plants, the transgene was a genomic sequence expressed from the native promoter. RT-PCR gave no evidence of increased AtKRP125c message levels in these plants (Fig. 2). Therefore, the disparate localization differences may reflect a real distinction between kinesin-5 motors in plants and animals.

Conclusion

In animals and fungi, it is well established that the organization of the bipolar spindle and the correct segregation of the chromosomes depends on a balance of forces exerted by motor proteins. The plus-end-directed kinesin-5 motor pushes and cortical dynein pulls on the spindle halves to provide an outward, poleward force, which is opposed by the inward force generated by minus-end-directed kinesin-14 motors (Sharp et al., 2000b). In plants, although a balance of forces within the spindle seems axiomatic, the responsible motors have remained unidentified. The absence of centrosomes and dynein and the proliferation of kinesins provides scope, in principle, for novelty in the force-generating machinery. However, the similarities in the phenotypes of kinesin-5-defective cells in animals, fungi and plants reveal that the function of this motor in spindle architecture has been strongly conserved across phyla.

Materials and Methods

Plant material and microtubule-inhibitor experiments

Arabidopsis thaliana (L.) Heynh was grown under constant conditions on a modified Hoagland's medium, as described elsewhere (Bannigan et al., 2006). All genotypes studied were in the Columbia background. For experiments with inhibitors, 1-week-old seedlings were transplanted onto plates containing medium supplemented with the test compound and returned to the growth chamber for 48 hours, when maximal root diameter was measured with the aid of a compound microscope, as described previously (Baskin et al., 2004). The compounds chosen, oryzalin and RH-4032 (Young and Lewandowski, 2000), were stored at –20°C as stock solutions in DMSO. Control plates were supplemented with 0.1% (v/v) DMSO, the highest amount of solvent used for any treatment.

Gene mapping, complementation and GFP constructs

A set of eight microsatellite markers placed *RSW7* between SSLP markers ciw39 and ciw40. A candidate gene, *At2g28620* was identified and sequenced. A single nucleotide polymorphism was found in the *rsw7* mutant which destroys a *Bsl*I restriction site in *At2g28620*, thereby providing a CAPS marker for genotyping. For complementation, an 11.8 kb genomic *Apa*I fragment from BAC T8O18 (nucleotides 44774-56586), spanning the AtKRP125c locus was cloned into a modified pCAMBIA3300 binary T-DNA vector (McElroy et al., 1995), introduced into *rsw7* plants by *Agrobacterium*-mediated transformation. To make an AtKRP125c-GFP reporter, a GFP sequence was inserted in frame into a *Sal*I site, eight codons upstream of the stop codon in the above 11.8 kb *Apa*I fragment. This removed six residues from the C terminus of AtKRP125c. The resulting construct was cloned and plants were transformed as described above, fully complementing the phenotype of *rsw7* plants.

The GFP-tubulin reporter lines express GFP fused to the *A. thaliana* β-tubulin-6 gene and were made by David Ehrhardt (Carnegie Institution, Stanford, CA), as previously described for the *A. thaliana* α-tubulin-5 gene (Shaw et al., 2003). Two transgenic lines expressing the GFP-tubulin reporter in the Columbia background, representing independent transformants with the same construct, were crossed onto *rsw7*. Lines homozygous for *rsw7* and brightly fluorescent were selected by visual inspection from the F2 and bulked up.

Immunofluorescence and observation of GFP reporters

Seven-day-old seedlings were fixed as described elsewhere (Bannigan et al., 2006). For microtubule labeling, we used 1:1000 monoclonal mouse anti-α-tubulin antibody (Sigma, St Louis, MO) or, for double labeling experiments, 1:200 rabbit polyclonal anti-α-tubulin (Cyr et al., 1987). The secondary antibody used for microtubules was 1:200 goat anti-mouse CY3 (Jackson ImmunoResearch, West Chester, PA) or, for double labeling, 1:100 goat anti-rabbit Alexa Fluor 488 (Invitrogen, Carlsbad, CA). Seedlings double-labeled for microtubules and DNA were labeled with 1:200 goat anti-mouse CY2 secondary antibody (Jackson), rinsed, and treated with 1 μg/ml RNAse A for 1 hour at 37°C, rinsed, and stained with 3 μM propidium iodide for 1 hour at room temperature. Plants double-labeled for microtubules and γ-tubulin were labeled with the above double labeling antibodies and 1:500 mouse monoclonal G9 anti-γ-tubulin primary antibody (Horio et al., 1999). Seedlings expressing GFP reporters were imaged as described previously (Bannigan et al., 2006).

RT-PCR analysis of AtKRP125c

Entire, 2-week-old seedlings were harvested from plates, frozen, and ground to a fine powder under liquid nitrogen with a cooled mortar and pestle. RNA was extracted using Qiagen RNeasy Plant Mini Kits, according to the manufacturer's instructions. cDNA was generated from 4 μg RNA using Superscript First Strand Synthesis Kit for RT-PCR (Invitrogen), with oligo(dT) as a primer. Primers RSW7RT F, R (supplementary material Table S1) were designed to amplify a small section of the *AtKRP125c* gene (279 bp from genomic DNA, 198 bp from cDNA), from both the native copy and the transgene, and expression levels were compared. As a loading control, primers specific to elongation factor 1α (EF1α) were used.

AtKRP125c-myc construct

The approximate 5′ end of the AtKRP125c mRNA was identified by screening a series of overlapping 5′ oligonucleotides for the ability to prime amplification of the cDNA from oligo(dT)-primed first-strand cDNA derived from leaf mRNA. A 3325 bp cDNA was then amplified using the most distal 5′ primer (RSW7myc F; supplementary material Table S1) that produced a product and 3′ primer (RSW7myc R). The PCR product was cloned into pCR-XL-TOPO using the Invitrogen XL cloning kit to produce pCRXL-TOPO rc-RSW-7@1. Sequencing this clone revealed that it encoded a 3126 bp reading frame that was 102 bp shorter than the predicted cDNA in TAIR, due to splicing of an unpredicted intron.

Primers [RSW7(NotI) F, R; supplementary material Table S1] were designed to amplify AtKRP125c out of the vector introducing a *Not*I restriction site on either end. PCR was performed using PFU polymerase (Stratagene), and A overhangs were added by incubating with dNTPs and Taq polymerase at 72°C for 25 minutes. The product was purified using a Qiaquick PCR purification kit (Qiagen), ligated into gateway vector pGEM according to the pGEM kit instructions (Promega) and transformed into DH5α-competent *E. coli* cells. Colonies were screened for the insertion by digesting with *Not*I and *Bgl*I. The PCR product was sequenced out of pGEM using universal M13 primers and primers designed every 500-600 base pairs within the cDNA (RSW7SEQ1-4, supplementary material Table S1). No mutations were introduced during PCR. The insert was gel purified and ligated into *Not*I-digested and SAP-treated pCMV-Myc (Clontech), then transformed into DH5α cells. The cells were screened for insertions in the correct orientation by digesting with *Eco*RI. A Qiagen endo-free plasmid purification kit was used to isolate the DNA, which was used for transfecting animal cells.

Animal cell culture, transfection, fixing and immunolabeling

Porcine kidney epithelial cells, LLC-Pk1 (American Type Culture Collection, Manassas, VA) were grown at 37°C and 5% CO_2 in a 1:1 mix of Ham's F10 and OptiMEM supplemented with 7.5% fetal calf serum and antibiotic and antimycotic. For observation, cells were plated on 22 mm coverslips and allowed to grow for 24 hours before transfecting.

For knockdown of Eg5 in LLC-Pk1 cells, we used a previously published siRNA sequence (Weil et al., 2002) and modified it for small hairpin RNA according to the method of Brummelkamp et al. (Brummelkamp et al., 2002). The Eg5 hairpin was inserted into pG-SHIN2 vector [a kind gift from S. Kojima (Kojima et al., 2004)].

For transfection with the AtKRP125c:myc construct or the Eg5 hairpin construct, we used Lipofectamine 2000 (Invitrogen) according to the manufacturer's instructions. Cells were allowed to recover for 2 days before fixing and immunolabeling. Cells treated with monastrol were incubated in 200 μM monastrol for 1 hour immediately before fixing.

Before fixing, cells were rinsed twice in Ca^{2+}- and Mg^{2+}-free PBS, then rinsed for 8 seconds in Karsenti's extraction buffer (80 mM Pipes, 5 mM EGTA, 1 mM $MgSO_4$, 0.5% Triton X-100). Cells were then fixed in –20°C methanol for 10 minutes, rehydrated in Ca^{2+}- and Mg^{2+}-free PBS containing 0.1% Tween 20 and 0.02% sodium azide (PBS-tw-azide). Cells were incubated in equal parts of primary antibody [anti-α-tubulin, YL1/2 (rat), Accurate Chemical, Westbury, NY; anti-Myc (mouse) Clontech; anti-Eg5 (rabbit), a generous gift from Duane Compton, Dartmouth Medical School, Hanover, NH (Mountain et al., 1999)] and 2% BSA for 1 hour at 37°C, rinsed in PBS-Tw-Azide and incubated with secondary antibodies (anti-rat FITC, anti-rabbit CY3, anti-mouse Alexa Fluor 633). Cells were mounted in Vectashield (Vector Laboratories, Burlingame, CA) and sealed with clear nail polish.

References

Ambrose, J. C., Li, W., Marcus, A., Ma, H. and Cyr, R. (2005). A minus-end-directed kinesin with plus-end tracking protein activity is involved in spindle morphogenesis. *Mol. Biol. Cell* **16**, 1584-1592.

Asada, T., Sonobe, S. and Shibaoka, H. (1991). Microtubule translocation in the cytokinetic apparatus of cultured tobacco cells. *Nature* **350**, 238-241.

Asada, T., Kuriyama, R. and Shibaoka, H. (1997). TKRP125, a kinesin-related protein involved in the centrosome-independent organization of the cytokinetic apparatus in tobacco BY-2 cells. *J. Cell Sci.* **110**, 179-189.

Bannigan, A., Wiedemeier, A. M., Williamson, R. E., Overall, R. L. and Baskin, T. I. (2006). Cortical microtubule arrays lose uniform alignment between cells and are oryzalin resistant in the *Arabidopsis* mutant, *radially swollen 6*. *Plant Cell Physiol.* **47**, 949-958.

Barroso, C., Chan, J., Allan, V., Doonan, J., Hussey, P. and Lloyd, C. (2000). Two kinesin-related proteins associated with the cold-stable cytoskeleton of carrot cells: characterization of a novel kinesin, DcKRP120-2. *Plant J.* **24**, 859-868.

Baskin, T. I. and Cande, W. Z. (1990). The structure and function of the mitotic spindle in flowering plants. *Annu. Rev. Plant Physiol. Plant Mol. Biol.* **41**, 277-315.

Baskin, T. I., Beemster, G. T. S., Judy-March, J. E. and Marga, F. (2004). Disorganization of cortical microtubules stimulates tangential expansion and reduces

the uniformity of cellulose microfibril alignment among cells in the root of Arabidopsis. *Plant Physiol.* **135**, 2279-2290.

Binarová, P., Dolezel, J., Draber, P., Heberle-Bors, E., Strnad, M. and Bögre, L. (1998). Treatment of *Vicia faba* root tip cells with specific inhibitors to cyclin-dependent kinases leads to abnormal spindle formation. *Plant J.* **16**, 697-707.

Blangy, A., Lane, H. A., d'Herin, P., Harper, M., Kress, M. and Nigg, E. A. (1995). Phosphorylation by p34cdc2 regulates spindle association of human Eg5, a kinesin-related motor essential for bipolar spindle formation in vivo. *Cell* **83**, 1159-1169.

Brown, R. C. and Lemmon, B. E. (2001). The cytoskeleton and spatial control of cytokinesis in the plant life cycle. *Protoplasma* **215**, 35-49.

Brown, R. C., Lemmon, B. E. and Horio, T. (2004). Gamma-tubulin localisation changes from discrete polar organizers to anastral spindles and phragmoplasts in mitosis of *Marchantia polymorpha* L. *Protoplasma* **224**, 187-193.

Brummelkamp, T. R., Bernards, R. and Agami, R. (2002). A system for stable expression of short interfering RNAs in mammalian cells. *Science* **296**, 550-553.

Cyr, R. J., Bustos, M. M., Guiltinan, M. J. and Fosket, D. E. (1987). Developmental modulation of tubulin protein and mRNA levels during somatic embryogenesis in cultured carrot cells. *Planta* **171**, 365-376.

DeBonis, S., Simorre, J.-P., Crevel, I., Lebeau, L., Skoufias, D. A., Blangy, A., Ebel, C., Gans, P., Cross, R., Hackney, D. D. et al. (2003). Interaction of the mitotic inhibitor monastrol with human kinesin Eg5. *Biochemistry* **42**, 338-349.

Dibbayawan, T. P., Harper, J. D. I. and Marc, J. (2001). A γ-tubulin antibody against a plant peptide sequence localises to cell division-specific microtubule arrays and organelles in plants. *Micron* **32**, 671-678.

Endow, S. (1999). Microtubule motors in spindle and chromosome motility. *Eur. J. Biochem.* **262**, 12-17.

Gadde, S. and Heald, R. (2004). Mechanisms and molecules of mitotic spindle. *Curr. Biol.* **14**, R797-R805.

Goldstein, L. S. and Philp, A. V. (1999). The road less travelled: emerging principles of kinesin motor utilization. *Annu. Rev. Cell. Biol.* **15**, 141-183.

Heck, M. M., Pereira, A., Pesavento, P., Yannoni, Y., Spradling, A. C. and Goldstein, L. S. (1993). The kinesin-like protein KLP61F is essential for mitosis in *Drosophila*. *J. Cell Biol.* **123**, 665-679.

Horio, T., Basaki, A., Takeoka, A. and Yamato, M. (1999). Lethal level overexpression of γ-tubulin in fission yeast causes mitotic arrest. *Cell Motil. Cytoskeleton* **44**, 284-295.

Kapitein, L. C., Peterman, E. J. G., Kwok, B. H., Kin, J. H., Kapoor, T. M. and Schmidt, C. F. (2005). The bipolar mitotic kinesin Eg5 moves on both microtubules that it crosslinks. *Nature* **435**, 114-118.

Kapoor, T. M., Mayer, T. U., Coughlin, M. L. and Mitchison, T. J. (2000). Probing spindle assembly mechanisms with monastrol, a small molecule inhibitor of the mitotic kinesin, Eg5. *J. Cell Biol.* **150**, 975-988.

Katsaros, C., Karyophyllis, D. and Galatis, B. (2006). Cytoskeleton and morphogenesis in brown algae. *Ann. Bot.* **97**, 679-693.

Kojima, S., Vignjevic, D. and Borisy, G. G. (2004). Improved silencing vector co-expressing GFP and small hairpin RNA. *Biotechniques* **36**, 74-79.

Lawrence, C. J., Malmberg, R. L., Muszynski, M. G. and Dawe, R. K. (2002). Maximum likelihood methods reveal conservation of function among closely related kinesin families. *J. Mol. Evol.* **54**, 42-53.

Lee, Y.-R. J. and Liu, B. (2004). Cytoskeletal motors in Arabidopsis. Sixty-one kinesins and seventeen myosins. *Plant Physiol.* **136**, 3877-3883.

Liu, B., Marc, J., Joshi, H. C. and Palevitz, B. A. (1993). A γ-tubulin-related protein associated with microtubule arrays of higher plants in cell-cycle-dependent manner. *J. Cell Sci.* **104**, 1217-1228.

Maliga, Z. and Mitchison, T. J. (2006). Small molecule and mutational analysis of allosteric Eg5 inhibition by monastrol. *BMC Chem. Biol.* **6**, 2-10.

Mao, G., Chan, J., Calder, G., Doonan, J. H. and Lloyd, C. W. (2005). Modulated targeting of GFP-AtMAP65-1 to central spindle microtubules during division. *Plant J.* **43**, 469-478.

Marcus, A. I., Li, W., Ma, H. and Cyr, R. J. (2003). A kinesin mutant with an atypical bipolar spindle undergoes normal mitosis. *Mol. Biol. Cell* **14**, 1717-1726.

Mazia, D. (1984). Centrosomes and mitotic poles. *Exp. Cell Res.* **153**, 1-15.

McElroy, D., Chamberlain, D. A., Moon, E. and Wilson, K. J. (1995). Development of GUS reporter gene constructs for cereal transformation. *Mol. Breed.* **1**, 27-37.

Mineyuki, Y. (2007). Plant microtubule studies: past and present. *J. Plant Res.* **120**, 45-51.

Mountain, V., Simerly, C., Howard, L., Ando, A., Schatten, G. and Compton, D. A. (1999). The kinesin-related protein, HSET, opposes the activity of Eg5 and cross-links microtubules in the mammalian mitotic spindle. *J. Cell Biol.* **147**, 351-365.

O'Connell, M. J., Meluh, P. B., Rose, M. D. and Morris, N. R. (1993). Suppression of the bimC4 mitotic spindle defect by deletion of klpA, a gene encoding a KAR3-related kinesin-like protein in *Aspergillus nidulans*. *J. Cell Biol.* **120**, 153-162.

Peters, N. T. and Kropf, D. L. (2006). Kinesin-5 motors are required for organization of spindle microtubules in *Silvetia compressa* zygotes. *BMC Plant Biol.* **6**, 19-28.

Reddy, A. S. and Day, I. S. (2001). Kinesin in the *Arabidopsis* genome: a comparative analysis among eukaryotes. *BMC Genomics* **2**, 2-14.

Sawin, K. E. and Mitchison, T. J. (1995). Mutations in the kinesin-like protein Eg5 disrupting localisation to the mitotic spindle. *Proc. Natl. Acad. Sci. USA* **92**, 4289-4293.

Sawin, K. E., LeGuellec, K., Philippe, M. and Mitchison, T. J. (1992). Mitotic spindle organization by a plus-end-directed microtubule motor. *Nature* **359**, 540-543.

Sharp, D. J., McDonald, K. L., Brown, H. M., Matthies, H. J., Walczak, C., Vale, R. D., Mitchison, T. J. and Scholey, J. M. (1999). The bipolar kinesin, KLP61F, cross-links microtubules within interpolar microtubule bundles of *Drosophila* embryonic mitotic spindles. *J. Cell Biol.* **144**, 125-138.

Sharp, D. J., Rogers, G. C. and Scholey, J. M. (2000a). Microtubule motors in mitosis. *Nature* **407**, 41-47.

Sharp, D. J., Brown, H. M., Kwon, M., Rogers, G. C., Holland, G. and Scholey, J. M. (2000b). Functional coordination of three mitotic motors in *Drosophila* embryos. *Mol. Biol. Cell* **11**, 241-253.

Shaw, S. L., Kamyar, R. and Ehrhardt, D. W. (2003). Sustained microtubule treadmilling in *Arabidopsis* cortical arrays. *Science* **300**, 715-718.

Turner, J., Anderson, R., Guo, J., Beraud, C., Fletterick, R. and Sakowicz, R. (2001). Crystal structure of the mitotic spindle kinesin Eg5 reveals a novel conformation of the neck-linker. *J. Biol. Chem.* **276**, 25496-25502.

Vanstraelen, M., Van Damme, D., De Rycke, R., Mylle, E., Inzé, D. and Geelen, D. (2006). Mitosis-specific kinesins in arabidopsis. *Trends Plant Sci.* **11**, 167-175.

Wadsworth, P., Rusan, N. M., Tulu, U. S. and Fagerstrom, C. (2005). Stable expression of fluorescently tagged proteins for studies of mitosis in mammalian cells. *Nat. Methods* **2**, 981-987.

Weil, D., Garçon, L., Harper, M., Duménil, D., Dautry, F. and Kress, M. (2002). Targeting the kinesin Eg5 to monitor siRNA transfection in mammalian cells. *Biotechniques* **33**, 1244-1248.

Wiedemeier, A. M. D., Judy-March, J. E., Hocart, C. H., Wasteneys, G. O., Williamson, R. E. and Baskin, T. I. (2002). Mutant alleles of *Arabidopsis RADIALLY SWOLLEN4* and *7* reduce growth anisotropy without altering the transverse orientation of cortical microtubules or cellulose microfibrils. *Development* **129**, 4821-4830.

Young, D. H. and Lewandowski, V. T. (2000). Covalent binding of the benzamide RH-4032 to tubulin in suspension-cultured tobacco cells and its application in a cell-based competitive-binding assay. *Plant Physiol.* **124**, 115-124.